Journal of Computational Physics 541 (2025) 114349

Contents lists available at ScienceDirect

Journal of Computational Physics

journal homepage: www.elsevier.com/locate/jcp

Time-integration of Gaussian variational approximation for the magnetic Schrödinger equation

Malik Scheifinger [a,*], Kurt Busch [b,c], Marlis Hochbruck [a], Caroline Lasser [d]

[a] Institute for Applied and Numerical Mathematics, Karlsruhe Institute of Technology, Englerstr. 2, 76131, Karlsruhe, Germany
[b] Institut für Physik, Humboldt Universität zu Berlin, Newtonstr. 15, 12489, Berlin, Germany
[c] Max-Born-Institut, Max-Born-Str. 2A, 12489, Berlin, Germany
[d] Department of Mathematics, Technische Universität München, Boltzmannstr. 3, 85748, Garching b. München, Germany

ARTICLE INFO

2020 MSC:
37M15
81Q05
81-08
78M30
81Q20

Keywords:
Gaussian wave packets
Semiclassical magnetic Schrödinger equation
Time-dependent variational approximation
Mesh-free method
Boris algorithm
Runge–Kutta
Penning trap

ABSTRACT

In the present paper we consider the semiclassical magnetic Schrödinger equation, which describes the dynamics of charged particles under the influence of an electro-magnetic field. The solution of the time-dependent Schrödinger equation is approximated by a single Gaussian wave packet via the time-dependent Dirac–Frenkel variational principle. For the approximation we use ordinary differential equations of motion for the parameters of the variational solution and extend the second-order Boris algorithm for classical mechanics to the quantum mechanical case. In addition, we propose a modified version of the classical fourth-order Runge–Kutta method. Numerical experiments explore parameter convergence and geometric properties. Moreover, we benchmark against the analytical solution of the Penning trap.

1. Introduction

In the present paper, we study the numerical time-integration for charged quantum particles that are subjected to external magnetic and electric fields. The dynamics is governed by the semiclassical magnetic Schrödinger equation

$$\mathrm{i}\varepsilon\partial_t\psi(t) = H(t)\psi(t), \quad \psi(0) = \psi_0, \quad t \in \mathbb{R}, \tag{1.1a}$$

on $\mathbb{R}^d$ with magnetic Hamiltonian

$$H(t) = \frac{1}{2}\left(-\mathrm{i}\varepsilon\nabla_x - A(t,\cdot)\right)^2 + \phi(t,\cdot), \tag{1.1b}$$

and initial value $\psi_0 \in L^2(\mathbb{R}^d)$ with semiclassical parameter $0 < \varepsilon \ll 1$. Here, A is a divergence-free magnetic vector potential, and ϕ is the electric potential. From a numerical point of view, solving this time-dependent partial differential equation raises three major problems. First, it is a high-dimensional problem, since the space dimension is typically given by $d = 3N$, where N is the number of

* Corresponding author.
E-mail addresses: malik.scheifinger@kit.edu (M. Scheifinger), kurt.busch@physik.hu-berlin.de (K. Busch), marlis.hochbruck@kit.edu (M. Hochbruck), classer@tum.de (C. Lasser).

https://doi.org/10.1016/j.jcp.2025.114349
Received 11 April 2025; Received in revised form 4 July 2025; Accepted 2 September 2025
Available online 5 September 2025

quantum particles in the system. Further, the computational domain $\mathbb{R}^d$ is naturally unbounded, and thus most numerical methods require truncation before discretization. For the method of lines (first discretize space, then time), high dimension combined with an unbounded domain leads to inadequately, if not intractably, large systems that have to be integrated in time. Another challenge is given by the high oscillations induced by the small semiclassical parameter ϵ. For standard time integration schemes, severe step-size restrictions have to be imposed and leave these methods impracticable.

We consider the case that the initial condition ψ_0 is strongly localized and given by a Gaussian wave packet, and investigate the numerical time-integration of an approximate solution $u \approx \psi$, which is a Gaussian wave packet

$$u(t,x) = \exp\Big(\frac{\mathrm{i}}{\epsilon}\big(\frac{1}{2}(x-q_t)^\top C_t(x-q_t) + (x-q_t)^\top p_t + \zeta_t\big)\Big).$$

The parameters to be computed are the packet's position and momentum center q_t, p_t, the complex width matrix C_t of the envelope, and the complex phase and weight parameter ζ_t. These parameters evolve according to ordinary differential equations, which are systematically derived by the Dirac–Frenkel time-dependent variational principle. By the approximation ansatz, high oscillations in time and space are captured and thus eliminated for the numerical time integration. For $A = 0$ it is well established that variational Gaussian wave packets offer reasonable mesh-free approximations at low computational cost, see for example [1,2]. More recently, they have also been proposed for magnetic quantum dynamics [3].

1.1. Contributions of the paper

As our main contribution, we derive two fast algorithms to solve the equations of motion for the parameters of a variational Gaussian wave packet approximation such that norm and energy conservation of the quantum solution are reflected by excellent long-time norm and energy accuracy of the time integrator. On a standard laptop with a non-optimized Jupyter Notebook[1], these algorithms enable us to compute approximations within minutes. First, we suggest an extension of the Boris algorithm [4,5], which is a standard integrator for the classical equations of motion for a charged particle system in plasma physics, to the quantum mechanical setting. We furthermore modify the well-known Runge–Kutta 4 method, such that it conserves the L^2-norm of a Gaussian wave packet at every time step. Numerical experiments in two and three space dimensions underline the efficiency and expected accuracy of the proposed algorithms.

1.2. Outline of the paper

The paper is structured as follows. In Section 2, we discuss the quantum dynamics of an electron and a proton in a hyperbolic Penning trap as a guiding example for a magnetic Schrödinger equation in the semiclassical regime. In Section 3, we compare variational and traditional Gaussian wave packet approximations and review the known error estimates. In Section 4, we transform the system of ordinary differential equations that determine the variational parameter evolution in a form that features averaged magnetic momenta and contains the magnetic vector field $B = \nabla \times A$ on the right-hand side. In particular, we derive an equation for the imaginary part of the phase parameter ζ guaranteeing the preservation of the L^2-norm. In Section 5, we briefly introduce the Boris algorithm used and derive our two algorithms for solving the parameters ODEs for the approximating Gaussian wave packet. Finally, in Section 6, we present numerical experiments for a two-dimensional magnetic system with trigonometric potentials and for the three-dimensional Penning trap. Appendix A gives formulas for the magnetic energy and other averages of Gaussian wave packets.

1.3. Notation

For a scalar function $a\colon \mathbb{R}^d \to \mathbb{R}$ we denote the Hessian matrix by $\nabla^2 a(x)$ and for a vector field $A\colon \mathbb{R}^d \to \mathbb{R}^d$ we denote the Jacobi matrix by $J_A(x) = (\partial_\ell A_k(x))_{k,\ell=1}^d$. For a function $W\colon \mathbb{R}^d \to \mathbb{R}^L$, $L \geq 1$, and more generally a linear operator $\mathbf{A}$ acting on $L^2(\mathbb{R}^d)$ we define the averages

$$\langle W\rangle_u := \langle u|Wu\rangle, \quad \langle \mathbf{A}\rangle_u := \big\langle u|\mathbf{A}u\big\rangle,$$

if the inner products exist. We follow the convention that inner products are anti-linear in the first component. We also use the dot product of vectors $v, w \in \mathbb{C}^L$ as $v \cdot w := v^\top w = v_1 w_1 + \cdots + v_L w_L$ and the square $v^2 := v \cdot v$. For complex matrices $C \in \mathbb{C}^{d\times d}$ we denote the component-wise real and imaginary parts by $C_\mathrm{R}, C_\mathrm{I} \in \mathbb{R}^{d\times d}$, respectively.

2. Penning trap

To illustrate semiclassical scaling for magnetic quantum dynamics we consider a charged microscopic particle, e.g., an electron or a proton, in a macroscopic hyperbolic Penning trap. Such a trap consists of an arrangement of magnetic coils and electrodes which

[1] Codes available at https://gitlab.kit.edu/malik.scheifinger/magnschroedti.

Table 1
Typical frequencies for the undulatory motion of electrons and protons in a Penning trap, cf. [6, Tables 1 and 2].

Quantity	Electron	Proton
δ (Trap Size)	0.00335 m	0.00112 m
B_0 (Magnetic Field)	5.872 T	5.050 T
ϕ_0 (Electrode Potential)	10.22 V	53.10 V
$\nu_+ = \frac{\omega_+}{2\pi}$ (Corrected Cyclotron Frequency)	164.38 GHz	76.299 MHz
$\nu_3 = \frac{\omega_3}{2\pi}$ (Axial Frequency)	63.698 MHz	10.134 MHz
$\nu_- = \frac{\omega_-}{2\pi}$ (Magnetron Frequency)	12.341 kHz	672.93 kHz

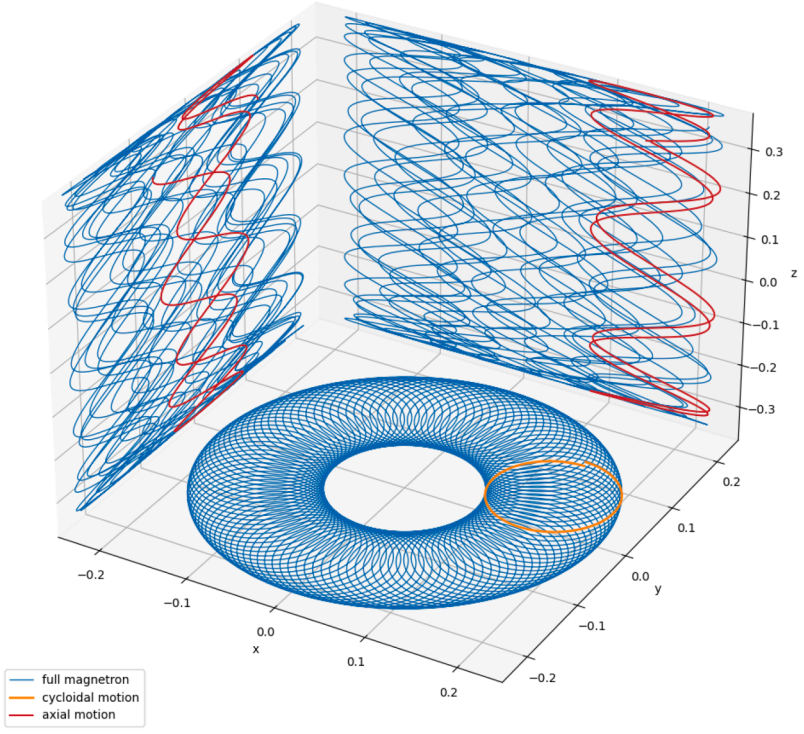

Fig. 1. Exact trajectory of a proton in a hyperbolic Penning trap with data from Table 1 and initial condition specified in Section 6.2 on the dimensionless time interval $[0, 2\pi]$.

feature a static magnetic field along the x_3-direction and a quadrupole-like static electric field that is rotationally symmetric around the x_3-axis, see, e.g., [6,7]. The corresponding vector and scalar potentials, respectively, read as

$$A(x) = \frac{1}{2} B_0 \begin{pmatrix} -x_2 \\ x_1 \\ 0 \end{pmatrix} \quad \text{and} \quad \phi(x) = \frac{\phi_0}{2\delta^2}\left(x_3^2 - \frac{1}{2}\left(x_1^2 + x_2^2\right)\right), \tag{2.1}$$

see Table 1 for typical trap parameters B_0, ϕ_0, δ for protons and electrons. A classical point particle (mass m, charge q_e) moving in such an electromagnetic field configuration executes an oscillatory motion along the x_3-axis (angular frequency ω_3), while simultaneously executing an epicyclic motion in the x_1x_2-plane where the low-frequency magnetron orbit (magnetron frequency ω_-) is overlaid with high-frequency cyclotron orbits (angular frequency ω_+), cf. Fig. 1. In terms of the particle and trap parameters, these frequencies are given by

$$\omega_\pm = \frac{1}{2}\left(\omega_c \pm \Omega\right), \quad \omega_3 = \sqrt{\frac{|q_e|\phi_0}{m\delta^2}}, \quad \text{where} \quad \omega_c = \frac{|q_e|B_0}{m}, \quad \Omega = \sqrt{\omega_c^2 - 2\omega_3^2}.$$

The associated classical trajectories $x_c(t)$ may be obtained via Newtonian [6] or Hamiltonian [8] approaches.

The quantum dynamics of a trapped particle is governed by the time-dependent Schrödinger equation which, in SI units, reads

$$\mathrm{i}\hbar\,\partial_t\psi(t,x) = \left(\frac{1}{2m}\left(-\mathrm{i}\hbar\nabla_x - q_e A(x)\right)^2 + q_e\phi(x)\right)\psi(t,x). \tag{2.2}$$

A first comparison of the macroscopic spatial extent of the trap, described by the trap parameter $\delta \approx 1$mm, with the wavelength of the trapped quantum particle (e.g., a proton) corresponding to the corrected cyclotron frequency $\nu_+ \approx 76$MHz indicates already that

mesh-based approaches to Eq. (2.2) are rather impracticable. Upon transiting to dimensionless coordinates $x \to x/\delta$ and introducing the dimensionless time $t \to \omega_- t$, Eq. (2.2) becomes

$$\mathrm{i}\varepsilon \partial_t \psi(t,x) = \left(\frac{1}{2}\big(\mathrm{i}\varepsilon\nabla + A_m(x)\big)^2 + \operatorname{sign}(q_e)\frac{\omega_+}{\omega_-}\left(x_3^2 - \frac{1}{2}\big(x_1^2 + x_2^2\big)\right)\right)\psi(t,x). \tag{2.3}$$

This is of the form Eq. (1.1), since with the effective magnetron magnetic field $B_m = m\omega_-/q_e$ we obtain the scaled dimensionless quantities

$$\varepsilon = \hbar/(q_e B_m \delta^2) \approx 1.19 \cdot 10^{-8}, \quad \omega_+/\omega_- \approx 113.25,$$

$$A_m(x) = \frac{1}{2}\frac{B_0}{B_m}\begin{pmatrix} -x_2 \\ x_1 \\ 0 \end{pmatrix}, \quad \frac{B_0}{B_m} \approx 114.25.$$

Since the semiclassical parameter $\varepsilon \approx 1.19 \cdot 10^{-8}$ is very small, the dynamics of the wave function are highly oscillatory in space and time, motivating the Gaussian wave packet ansatz Eq. (3.1) for eliminating high oscillations. In Fig. 1, we illustrate the corresponding proton dynamics for the typical trap parameters of Table 1. The parameters of the initial Gaussian wave packet $\psi(0,x)$ are specified in Eq. (6.3). The plot depicts the exact trajectory of the center in blue. One cycle of the cycloidal motion is highlighted in orange and one of the axial motion in red.

3. Variational approximation

In the semiclassical regime, the solution of the Schrödinger Eq. (1.1a) is highly oscillatory and well localized. We thus seek approximations within the manifold of complex Gaussian wave packets

$$\mathcal{M} = \Big\{ u \in L^2(\mathbb{R}^d) \;\Big|\; u(x) = \exp\Big(\frac{\mathrm{i}}{\varepsilon}\big(\frac{1}{2}(x-q)^\top C(x-q) + (x-q)^\top p + \zeta\big)\Big), \\ q,\, p \in \mathbb{R}^d,\, C = C^\top \in \mathbb{C}^{d\times d},\, \operatorname{Im} C \text{ positive definite}, \zeta \in \mathbb{C}\Big\}. \tag{3.1}$$

We construct the optimal approximation $u(t) \approx \psi(t)$, $u(t) \in \mathcal{M}$, in the sense that the time-derivative $\partial_t u(t)$ minimizes the residual,

$$\big\|\mathrm{i}\varepsilon \partial_t u(t) - H(t)u(t)\big\|_{L^2} = \min_{\partial_t u(t)}! \tag{3.2}$$

We consider initial data with $\psi_0 = u_0 \in \mathcal{M}$ and $\|u_0\|_{L^2} = 1$, and mention in passing, that the variational approximation Eq. (3.2) is norm preserving in any case and energy preserving for time-independent Hamiltonians,

$$\|u(t)\|_{L^2} = \|u_0\|_{L^2}, \quad \langle H\rangle_{u(t)} = \langle H\rangle_{u_0} \quad \text{for all } t,$$

see [9, §II.1.5].

3.1. Variational equations of motion

In earlier work [3], we derived ordinary differential equations for the parameters q_t, p_t, C_t, ζ_t of the approximating Gaussian wave packet, which we reproduce here. We denote the classical Hamiltonian function for charged particles in a magnetic field by

$$h(t,x,\xi) = \frac{1}{2}(\xi - A(t,x))^2 + \phi(t,x), \quad (t,x,\xi) \in \mathbb{R}\times\mathbb{R}^d\times\mathbb{R}^d.$$

Then, the residual minimization in Eq. (3.2) implies that

$$\dot q = \langle \partial_\xi h\rangle_u, \quad \dot p = -\langle \partial_x h\rangle_u, \quad \dot C = -\mathcal{B}(C), \tag{3.3a}$$

$$\dot\zeta = -\langle h\rangle_u + \frac{\varepsilon}{4}\operatorname{tr}\big(\mathcal{B}(C)C_{\mathrm{I}}^{-1}\big) + p^\top\langle \partial_\xi h\rangle_u, \tag{3.3b}$$

where the complex matrix $\mathcal{B}(C) \in \mathbb{C}^{d\times d}$, that depends on a Gaussian average, is given by

$$\mathcal{B}(C) = \begin{pmatrix}\mathrm{Id} & C\end{pmatrix}\langle \nabla^2 h\rangle_u \begin{pmatrix}\mathrm{Id} \\ C\end{pmatrix}. \tag{3.3c}$$

The averages $\langle \partial^\alpha h\rangle_u = \langle \operatorname{op}_{\mathrm{Weyl}}(\partial^\alpha h)\rangle_u$ use the standard Weyl quantization of the derivatives of the Hamiltonian function. In Section 4, we reformulate these averages such that the equations of motion become amenable to a Boris-type time discretization.

3.2. Asymptotic accuracy

The variational Gaussian wave packet $u(t)$ determined by Eq. (3.2) is the exact Schrödinger solution $\psi(t)$, if the magnetic potential $A(t,\cdot)$ is linear and the electric potential $\phi(t,\cdot)$ is quadratic with respect to position. In particular, the dynamics in a Penning trap are exactly described. More generally, if A and ϕ are sub-linear and sub-quadratic in the following sense,

$$\partial_x^\alpha A(t,\cdot), \quad \partial_x^\beta \phi(t,\cdot) \qquad \text{bounded for all } |\alpha| \geq 1,\ |\beta| \geq 2,$$

then the following bounds for the norm and the observable error can be proven, see [3, Theorems 3.8 & 3.10]. Given a finite time horizon $[0,T]$, the norm error and the observable error for expectation values with respect to a linear operator $\mathbf{A}$ satisfy

$$\|\psi(t)-u(t)\|_{L^2} \le c\,t\,\sqrt{\varepsilon}, \qquad \left|\langle \mathbf{A}\rangle_{\psi(t)} - \langle \mathbf{A}\rangle_{u(t)}\right| \le C\,t\,\varepsilon^2 \tag{3.4}$$

for all $t \in [0,T]$, where the constants $c, C > 0$ are independent from ε and t, but depend on a lower bound for the eigenvalues of C_{I} on $[0,T]$. It is worth pointing out the high observable accuracy.

3.3. Classical versus variational approximation

Traditional Gaussian wave packet approximation evolves the centers according to the purely classical equations of motion

$$\dot q = \partial_p h, \qquad \dot p = -\partial_q h,$$

see [10, §4]. If the magnetic and the electric potential are linear respectively quadratic in position (as they are for a Penning trap), then the classical and the variational approximation coincide and yield the exact quantum solution. For general Hamiltonians, however, the approximations differ. The variational equations of motion Eq. (3.3) contain averages with respect to the approximating Gaussian wave packet, which are computationally more costly than the pure point evaluations of the traditional approach. However, a traditional Gaussian approximation is neither energy preserving nor as accurate as a variational one, since the classical observable error is only first order in ε, while the variational one is second order.

3.4. Hagedorn parametrization

It is convenient to write the complex symmetric width matrix C in Hagedorn's parametrization as

$$C = C_{\mathrm{R}} + \mathrm{i}C_{\mathrm{I}} = PQ^{-1} \quad \text{and} \quad C_{\mathrm{I}} = (QQ^*)^{-1}, \tag{3.5}$$

with two real symmetric matrices $C_{\mathrm{R}}, C_{\mathrm{I}}$ and two invertible complex matrices Q, P that satisfy the symplecticity condition $Q^\top P - P^\top Q = 0$, $Q^*P - P^*Q = 2\mathrm{i}\mathrm{Id}$. Such a decomposition of complex symmetric matrices with positive definite imaginary part is unique up to unitary factors, see [9, Chapter V]. Unfortunately, we can express $C_{\mathrm{R}} = \frac{1}{2}(PQ^{-1} + (Q^*)^{-1}P^*)$ only in terms of both Q and P, which will have implications for the integrators to be developed. The matrices Q and P allow the efficient structure-preserving time-integration of the width matrix in parallel to the phase space center and give direct control of the wave packet's norm in terms of the matrix Q. In particular, the Riccati-type Eq. (3.3a) takes in Hagedorn's parametrization the form

$$\dot Q = \langle \partial_{pq} h\rangle_u Q + \langle \partial_{pp} h\rangle_u P, \quad \dot P = -\langle \partial_{qq} h\rangle_u Q - \langle \partial_{qp} h\rangle_u P.$$

These equations are variational analogues of the linearization of the classical equations of motion around a trajectory.

4. Transformation of equations of motion

We transform the variational equations of motion in such a way that they structurally mimic the classical equations for a charged particle.

4.1. Averaged magnetic momenta

In a first step, we rewrite the variational equations of motion such that an averaged version of the usual magnetic momenta becomes visible.

Lemma 4.1. *The variational equations of motion Eq. (3.3) for the parameters of a Gaussian wave packet are equivalent to*

$$\dot q = p - \langle A\rangle_u, \quad \dot p = \langle J_A^\top(\xi - A) - \nabla\phi\rangle_u, \tag{4.1a}$$

$$\dot C = -\langle \partial_x^2 h\rangle_u + \langle J_A^\top\rangle_u C + C\langle J_A\rangle_u - C^2, \tag{4.1b}$$

$$\dot\zeta = -\langle h\rangle_u + \frac{\varepsilon}{4}\mathrm{tr}\,(\mathcal{B}(C)C_{\mathrm{I}}^{-1}) + p^\top(p - \langle A\rangle_u), \tag{4.1c}$$

where $\langle a\rangle_u = \langle \mathrm{op}_{\mathrm{Weyl}}(a)\rangle_u$ for any smooth $a : \mathbb{R}^{2d} \to \mathbb{R}$, $(x,\xi) \mapsto a(x,\xi)$. In Hagedorn's parametrization, the matrix evolution Eq. (4.1b) satisfies

$$\dot Q = P - \langle J_A\rangle_u Q, \tag{4.2a}$$

$$\dot P = \langle J_A^\top\rangle_u P - \Big\langle J_A^\top J_A - \sum_{k=1}^{d} \nabla^2 A_k(\xi_k - A_k) + \nabla^2\phi\Big\rangle_u Q. \tag{4.2b}$$

Proof. Since the partial derivatives of the classical Hamiltonian function $h(x,\xi) = \frac{1}{2}(\xi - A(x))^2 + \phi(x)$ satisfy

$$\partial_\xi h(x,\xi) = \xi - A(x), \qquad \partial_x h(x,\xi) = -J_A(x)^\top(\xi - A(x)) + \nabla\phi(x),$$

we have Eq. (4.1a). We next turn to the second-order derivatives of h. Denoting the partial derivatives of the magnetic and the electric potential shortly by $\partial_1, \dots, \partial_d$, we have

$$\partial_{x_m}\partial_{x_\ell} h = \sum_{k=1}^{d} \big(\partial_m A_k \partial_\ell A_k - (\xi_k - A_k)\partial_m \partial_\ell A_k\big) + \partial_m \partial_\ell \phi,$$
$$\partial_{x_m}\partial_{\xi_\ell} h = -\partial_m A_\ell, \qquad \partial_{\xi_m}\partial_{x_\ell} h = -\partial_\ell A_m,$$

which gives a Hessian matrix

$$\nabla^2 h = \begin{pmatrix} \partial_x^2 h & \partial_{x\xi} h \\ \partial_{\xi x} h & \partial_\xi^2 h \end{pmatrix} = \begin{pmatrix} \partial_x^2 h & -J_A^\top \\ -J_A & \mathrm{Id} \end{pmatrix}$$

with $\partial_x^2 h = J_A^\top J_A - \sum_{k=1}^d \nabla^2 A_k(\xi_k - A_k) + \nabla^2\phi$. By Eq. (3.3c) we then infer that

$$\begin{aligned} \mathcal{B}(C) &= \langle \partial_x^2 h\rangle_u + \langle \partial_{x\xi} h\rangle_u C + C\langle \partial_{\xi x} h\rangle_u + C\langle \partial_\xi^2 h\rangle_u C \\ &= \langle \partial_x^2 h\rangle_u - \langle J_A^\top\rangle_u C - C\langle J_A\rangle_u + C^2. \end{aligned}$$

Hence, the variational equations of motion Eq. (3.3) are equivalent to Eq. (4.1). □

This formulation of the equations of motion prominently features averaged magnetic momenta

$$v := p - \langle A\rangle_u, \qquad \Upsilon := P - \langle J_A\rangle_u Q. \tag{4.3}$$

We aim at rewriting them in terms of the real vector $v(t) \in \mathbb{R}^d$ and the complex matrix $\Upsilon(t) \in \mathbb{C}^{d\times d}$.

4.2. Equations for the center and the width

Since the averaged magnetic momenta contain averages of the magnetic field and of its Jacobian, we need a compact way of assessing the time derivative of averages in the spirit of a magnetic Ehrenfest-type theorem.

Proposition 1. *For any smooth function $w\colon \mathbb{R}^d \to \mathbb{R}$, its average with respect to the variational Gaussian wave packet $u = u(t)$ satisfies*

$$\frac{d}{dt}\langle w\rangle_u = \langle \nabla w\rangle_u^\top v + \frac{\varepsilon}{2}\mathrm{tr}\big(\langle \nabla^2 w\rangle_u(\Upsilon Q^* - \mathrm{i}\mathrm{Id})\big),$$

where $\Upsilon Q^* - \mathrm{i}\mathrm{Id}$ is a real matrix.

Proof. We differentiate the position density with respect to time,

$$\begin{aligned} \partial_t |u(t,x)|^2 &= \partial_t \exp\Big(-\frac{1}{\varepsilon}(x-q)^\top C_\mathrm{I}(x-q) - \frac{2}{\varepsilon}\zeta_\mathrm{I}\Big) \\ &= |u(t,x)|^2\Big(-\frac{1}{\varepsilon}(x-q)^\top \dot C_\mathrm{I}(x-q) + \frac{2}{\varepsilon}(x-q)^\top C_\mathrm{I}\dot q - \frac{2}{\varepsilon}\dot\zeta_\mathrm{I}\Big) \\ &= |u(t,x)|^2\Big(\frac{2}{\varepsilon}(x-q)^\top\big(C_\mathrm{R} - \langle J_A^\top\rangle_u\big)C_\mathrm{I}(x-q) + \frac{2}{\varepsilon}(x-q)^\top C_\mathrm{I} v - \mathrm{tr}\,(C_\mathrm{R})\Big), \end{aligned}$$

where we have used that, by Lemma 4.1, the symmetry of C_R and C_I, and $\mathrm{tr}\,(\langle J_A\rangle_u) = 0$ since $\nabla\cdot A = 0$,

$$\dot q = v, \quad \dot C_\mathrm{I} = C_\mathrm{I}(\langle J_A\rangle_u - C_\mathrm{R}) + (\langle J_A^\top\rangle_u - C_\mathrm{R})C_\mathrm{I}, \quad \dot\zeta_\mathrm{I} = \frac{\varepsilon}{2}\mathrm{tr}\,(C_\mathrm{R}).$$

Therefore, we obtain

$$\begin{aligned} \frac{d}{dt}\langle w\rangle_u &= \frac{2}{\varepsilon}\Big\langle w(x-q)^\top\big(C_\mathrm{R} - \langle J_A^\top\rangle_u\big)C_\mathrm{I}(x-q)\Big\rangle_u \\ &\quad + \frac{2}{\varepsilon}\big\langle wC_\mathrm{I}(x-q)\big\rangle_u^\top v - \langle w\rangle_u \mathrm{tr}\,(C_\mathrm{R}) \\ &= \langle w\rangle_u \mathrm{tr}\,(C_\mathrm{R} - \langle J_A^\top\rangle_u) + \langle \nabla w\rangle_u^\top v - \langle w\rangle_u \mathrm{tr}\,(C_\mathrm{R}) \\ &\quad + \frac{\varepsilon}{2}\mathrm{tr}\,(\langle \nabla^2 w\rangle_u C_\mathrm{I}^{-1}(C_\mathrm{R} - \langle J_A^\top\rangle_u)) \\ &= \langle \nabla w\rangle_u^\top v + \frac{\varepsilon}{2}\mathrm{tr}\,(\langle \nabla^2 w\rangle_u C_\mathrm{I}^{-1}(C_\mathrm{R} - \langle J_A^\top\rangle_u)), \end{aligned} \tag{4.4}$$

where the second equation relies on Lemma A.1 with matrix $M = \big(C_\mathrm{R} - \langle J_A^\top\rangle_u\big)C_\mathrm{I}$ and the last equation on $\nabla\cdot A = 0$. It remains to express the occurring matrices in terms of Q and Υ. Using the properties of Hagedorn's parametrization from Section 3.4 yields

$$\begin{aligned} C_\mathrm{I}^{-1}C_\mathrm{R} &= \frac{1}{2}QQ^*(PQ^{-1} + (Q^*)^{-1}P^*) \\ &= \frac{1}{2}\big(Q(P^*Q + 2\mathrm{i}\mathrm{Id})Q^{-1} + QP^*\big) \\ &= Q(\Upsilon^* + Q^*\langle J_A^\top\rangle_u) + \mathrm{i}\mathrm{Id}. \end{aligned}$$

Hence we have $C_\mathrm{I}^{-1}(C_\mathrm{R} - \langle J_A^\top\rangle_u) = Q\Upsilon^* + \mathrm{i}\mathrm{Id}$, and use the trace identity $\mathrm{tr}\,(MN) = \mathrm{tr}\,(MN^*)$ for the real symmetric matrix $M = \langle \nabla^2 w\rangle_u$ and the real matrix $N = Q\Upsilon^* + \mathrm{i}\mathrm{Id}$. □

Equipped with an equation for the time evolution of averages, we can determine the variational equations of motion solely in terms of the averaged magnetic momenta.

Theorem 4.1. *We consider the averaged magnetic momenta Eq. (4.3) and denote the magnetic field $B = \nabla \times A$. The variational equations of motion for the Gaussian wave packet's center and width, Eqs. (4.1a) and (4.2), can be transformed as*

$$\dot{q} = v, \qquad \dot{v} = v \times \langle B \rangle_u + E, \tag{4.5a}$$

$$\dot{Q} = \Upsilon, \qquad \dot{\Upsilon} = \Upsilon \times \langle B \rangle_u + SQ, \tag{4.5b}$$

where the matrix

$$\Upsilon \times \langle B \rangle_u := (v_1 \times \langle B \rangle_u, \dots, v_d \times \langle B \rangle_u)$$

is given by the cross product of the column vectors $v_1, \dots, v_d$ of Υ with $\langle B \rangle_u$. The real vector field E satisfies

$$\begin{aligned} E = &-\langle \nabla \phi \rangle_u - \langle \partial_t A \rangle_u + \langle J_A^\top \rangle_u \langle A \rangle_u - \langle J_A^\top A \rangle_u \\ &+ \frac{\varepsilon}{2} \Big(\operatorname{tr} \big(\langle \partial_k J_A^\top - \nabla^2 A_k \rangle_u (\Upsilon Q^* - \mathrm{i}\mathrm{Id}) + \langle \partial_k J_A^\top \rangle_u \langle J_A \rangle_u Q Q^* \big) \Big)_{k=1}^d, \end{aligned}$$

and the real matrix potential S can be written as

$$\begin{aligned} S = &-\langle \nabla^2 \phi \rangle_u - \langle J_{\partial_t A} \rangle_u + \langle J_A^\top \rangle_u \langle J_A \rangle_u - \langle J_A^\top J_A \rangle_u \\ &+ \sum_{m=1}^d \Big(\langle \nabla^2 A_m \rangle_u \langle A_m \rangle_u - \langle (\nabla^2 A_m) A_m \rangle_u + \big(\langle \partial_k \partial_\ell A_m - \partial_m \partial_\ell A_k \rangle_u v_m \big)_{k,\ell=1}^d \Big) \\ &+ \frac{\varepsilon}{2} \big(\operatorname{tr} \big(\langle \partial_k \partial_\ell J_A^\top - \nabla^2 \partial_\ell A_k \rangle_u (\Upsilon Q^* - \mathrm{i}\mathrm{Id}) + \langle \partial_k \partial_\ell J_A^\top \rangle_u \langle J_A \rangle_u Q Q^* \big) \big)_{k,\ell=1}^d. \end{aligned}$$

Proof. By Eq. (4.1a), the time derivative of the magnetic momenta satisfies

$$\dot{v} = \dot{p} - \frac{d}{dt} \langle A \rangle_u = \langle J_A^\top (\xi - A) - \nabla \phi \rangle_u - \frac{d}{dt} \langle A \rangle_u. \tag{4.6}$$

Hence, we have to work on $\langle J_A^\top \xi \rangle_u$. By symbolic Weyl calculus, see for example [10, §2.4], we expand the operator of the product as

$$\operatorname{op}_{\mathrm{Weyl}}(J_A^\top \xi) = J_A^\top \operatorname{op}_{\mathrm{Weyl}}(\xi) + \frac{\mathrm{i}\varepsilon}{2} \operatorname{op}_{\mathrm{Weyl}}(\{J_A^\top, \xi\}) = J_A^\top (-\mathrm{i}\varepsilon \nabla),$$

where the last equation uses that $\nabla \cdot A = 0$ implies that $\{J_A^\top, \xi\} = -\sum_{k=1}^d \partial_{x_k} (J_A^\top) \partial_{\xi_k} \xi = -\sum_{k=1}^d \partial_{x_k} \nabla A_k = 0$. Therefore,

$$\langle J_A^\top \xi \rangle_u = \langle u, J_A^\top (-\mathrm{i}\varepsilon \nabla) u \rangle = \langle J_A^\top C (x - q) \rangle_u + \langle J_A^\top \rangle_u p$$

due to $-\mathrm{i}\varepsilon \nabla u(x) = (C(x-q) + p) u(x)$. Then, we apply Lemma A.1 with $W = J_A^\top C$,

$$\begin{aligned} \langle J_A^\top C (x - q) \rangle_u &= \frac{\varepsilon}{2} \sum_{\ell=1}^d \big(\big(\langle \partial_\ell J_A^\top \rangle_u C C_{\mathrm{I}}^{-1} \big)_{k\ell} \big)_{k=1}^d \\ &= \frac{\varepsilon}{2} \sum_{m,\ell=1}^d \big(\langle \partial_\ell \partial_k A_m \rangle_u \big(\Upsilon Q^* + \langle J_A \rangle_u Q Q^* - \mathrm{i}\mathrm{Id} \big)_{m\ell} \big)_{k=1}^d \\ &= \frac{\varepsilon}{2} \big(\operatorname{tr} (\langle \partial_k J_A \rangle_u^\top (\Upsilon Q^* - \mathrm{i}\mathrm{Id} + \langle J_A \rangle_u Q Q^*) \big)_{k=1}^d, \end{aligned} \tag{4.7}$$

since $C C_{\mathrm{I}}^{-1} = (P Q^{-1})(Q Q^*) = (\Upsilon + \langle J_A \rangle_u Q) Q^*$ and $\operatorname{div} A = 0$. We thus obtain

$$\begin{aligned} \langle J_A^\top (\xi - A) \rangle_u = &\langle J_A^\top \rangle_u v + \langle J_A^\top \rangle_u \langle A \rangle_u - \langle J_A^\top A \rangle_u \\ &+ \frac{\varepsilon}{2} \big(\operatorname{tr} (\langle \partial_k J_A \rangle_u^\top (\Upsilon Q^* - \mathrm{i}\mathrm{Id} + \langle J_A \rangle_u Q Q^*) \big)_{k=1}^d. \end{aligned}$$

Now, we use Proposition 1 for each component of the magnetic potential,

$$\frac{d}{dt} \langle A \rangle_u = \langle \partial_t A \rangle_u + \langle J_A \rangle_u v + \frac{\varepsilon}{2} \Big(\operatorname{tr} \big(\langle \nabla^2 A_k \rangle_u (\Upsilon Q^* - \mathrm{i}\mathrm{Id}) \big) \Big)_{k=1}^d.$$

When collecting all the terms that originated in Eq. (4.6), we observe the occurrence of $\langle J_A^\top \rangle_u v$ and $-\langle J_A \rangle_u v$, which combine according to

$$\big\langle \big(J_A^\top - J_A \big) \big\rangle_u v = v \times \langle B \rangle_u.$$

We thus arrive at the claimed Eq. (4.5a). As for the matrix $\Upsilon = P - \langle J_A \rangle_u Q$, we use the equations of motion Eq. (4.2), which contain the average of $\partial_x^2 h = J_A^\top J_A - \sum_{m=1}^d \nabla^2 A_m (\xi_m - A_m) + \nabla^2 \phi$. We have

$$\dot{P} = \langle J_A^\top \rangle_u \big(\Upsilon + \langle J_A \rangle_u Q \big) - \langle \partial_x^2 h \rangle_u Q.$$

For computing $\langle \partial_x^2 h \rangle_u$, we observe that

$$\begin{aligned}\sum_{m=1}^{d} \mathrm{op}_{\mathrm{Weyl}}(\nabla^2 A_m \xi_m) &= \sum_{m=1}^{d} \Big(\nabla^2 A_m \mathrm{op}_{\mathrm{Weyl}}(\xi_m) + \frac{\mathrm{i}\epsilon}{2} \mathrm{op}_{\mathrm{Weyl}}\{\nabla^2 A_m, \xi_m\} \Big) \\ &= \sum_{m=1}^{d} \nabla^2 A_m(-\mathrm{i}\epsilon\partial_m),\end{aligned}$$

where the last equation uses that $\sum_{m=1}^{d} \{\nabla^2 A_m, \xi_m\} = 0$ due to $\nabla \cdot A = 0$. Arguing as for Eq. (4.7), we obtain

$$\begin{aligned}&\sum_{m=1}^{d} \langle \nabla^2 A_m (\xi_m - A_m) \rangle_u \\ &= \sum_{m=1}^{d} \big(\langle \nabla^2 A_m \big(C(x-q) \big)_m \rangle_u - \langle (\nabla^2 A_m) A_m \rangle_u + \langle \nabla^2 A_m \rangle_u p_m \big) \\ &= \sum_{m=1}^{d} \big(\langle \nabla^2 A_m \rangle_u \big(v_m + \langle A_m \rangle_u \big) - \langle (\nabla^2 A_m) A_m \rangle_u \big) \\ &\quad + \frac{\epsilon}{2} \sum_{m,n=1}^{d} \langle \nabla^2 \partial_n A_m \rangle_u \big(\Upsilon Q^* - \mathrm{i}\mathrm{Id} + \langle J_A \rangle_u Q Q^* \big)_{mn},\end{aligned}$$

and therefore

$$\begin{aligned}\langle \partial_x^2 h \rangle_u = \langle J_A^\top J_A + \nabla^2 \phi \rangle_u &- \sum_{m=1}^{d} \big(\langle \nabla^2 A_m \rangle_u \big(v_m + \langle A_m \rangle_u \big) - \langle (\nabla^2 A_m) A_m \rangle_u \big) \\ &- \frac{\epsilon}{2} \big(\mathrm{tr}\big(\langle \partial_k \partial_\ell J_A^\top \rangle_u \big(\Upsilon Q^* - \mathrm{i}\mathrm{Id} + \langle J_A \rangle_u Q Q^* \big) \big) \big)_{k,\ell=1}^{d}.\end{aligned} \tag{4.8}$$

We next use Proposition 1 applied to each component of the Jacobian matrix $J_A = (\partial_\ell A_k)_{k,\ell=1}^{d}$ and obtain

$$\begin{aligned}&\frac{d}{dt} \langle J_A \rangle_u = \langle J_{\partial_t A} \rangle_u \\ &+ \sum_{m=1}^{d} \big(\langle \partial_m \partial_\ell A_k \rangle_u v_m \big)_{k,\ell=1}^{d} + \frac{\epsilon}{2} \Big(\mathrm{tr}\Big(\langle \nabla^2 \partial_\ell A_k \rangle_u (\Upsilon Q^* - \mathrm{i}\mathrm{Id}) \Big) \Big)_{k,\ell=1}^{d}.\end{aligned}$$

Now we combine and arrive at

$$\dot{\Upsilon} = \dot{P} - \Big(\frac{d}{dt} \langle J_A \rangle_u \Big) Q - \langle J_A \rangle_u \dot{Q} = \langle J_A^\top - J_A \rangle_u \Upsilon + SQ$$

with the matrix potential S of the claimed form. □

Remark 1 (Linear potential A)**.** For a linear magnetic potential A, all higher order derivatives vanish and the average $\langle A \rangle_u = A(\cdot, q)$ is a point evaluation. Thus, the equations of motion of Lemma 4.1 simplify to

$$\dot{q} = v, \qquad \dot{v} = v \times B(q) - (\partial_t A(\cdot, q) + \langle \nabla \phi \rangle_u), \tag{4.9a}$$

$$\dot{Q} = \Upsilon, \qquad \dot{\Upsilon} = \Upsilon \times B(q) - (\partial_t J_A(\cdot, q) + \langle \nabla^2 \phi \rangle_u) Q. \tag{4.9b}$$

The Penning trap, see Sections 2 and 6.2, with its quadratic electric potential, has even simpler equations of motion, since also the averages of the electric potential collapse to $\langle \nabla \phi \rangle_u = \nabla \phi(\cdot, q)$ and $\langle \nabla^2 \phi \rangle_u = \nabla^2 \phi(\cdot, q)$.

4.3. Equations for the phase

The imaginary part of the complex parameter $\zeta = \zeta_{\mathrm{R}} + \mathrm{i}\zeta_{\mathrm{I}}$ carries the normalization of the Gaussian wave packet. We derive an explicit representation, which only depends on the determinant of the complex matrix Q. This representation will support our time discretization of ζ_{I} in Section 5.2.

Lemma 4.2. *For the real part $\zeta_{\mathrm{R}} = \mathrm{Re}\,(\zeta)$ we have*

$$\dot{\zeta}_{\mathrm{R}} = \frac{1}{2} v^2 + \langle A \rangle_u^\top v - \langle \phi \rangle_u + \frac{\epsilon}{4} \mathrm{tr}\,(\langle \partial_x^2 h \rangle_u Q Q^* - 2(Q Q^*)^{-1}), \tag{4.10a}$$

where the average $\langle \partial_x^2 h \rangle_u$ is given in Eq. (4.8) with respect to (q, v, Q, Υ). The imaginary part $\zeta_{\mathrm{I}} = \mathrm{Im}\,(\zeta)$ satisfies the normalization formula

$$\zeta_{\mathrm{I}}(t) = \zeta_{\mathrm{I}}(0) + \frac{\epsilon}{2} (\ln |\det Q(t)| - \ln |\det Q(0)|). \tag{4.10b}$$

Proof. We start with the normalization formula. Since $\operatorname{Im}\mathcal{B}(C) = -\langle J_A^\top\rangle_u C_\mathrm{I} - C_\mathrm{I}\langle J_A\rangle_u + C_\mathrm{R}C_\mathrm{I} + C_\mathrm{I}C_\mathrm{R}$ and $\operatorname{div}A = 0$, we have

$$\begin{aligned}\operatorname{Im}\left(\operatorname{tr}\left(\mathcal{B}(C)C_\mathrm{I}^{-1}\right)\right) &= 2\operatorname{tr}\left(C_\mathrm{R}\right) = 2\operatorname{tr}\left(\operatorname{Re}\left(PQ^{-1}\right)\right)\\ &= 2\operatorname{tr}\left(\operatorname{Re}\left((\dot Q + \langle J_A\rangle_u Q)Q^{-1}\right)\right)\\ &= 2\operatorname{tr}\left(\operatorname{Re}\left(\dot Q Q^{-1}\right)\right).\end{aligned}$$

We thus obtain from Eq. (4.1c) with Jacobi's formula

$$\begin{aligned}\dot\zeta_\mathrm{I} &= \frac{\varepsilon}{2}\operatorname{tr}\left(\operatorname{Re}\left(\dot Q Q^{-1}\right)\right)\\ &= \frac{\varepsilon}{4}\frac{1}{|\det Q|^2}\left(2\operatorname{Re}\left(\overline{\det Q}\det Q\ \operatorname{tr}\left(\dot Q Q^{-1}\right)\right)\right)\\ &= \frac{\varepsilon}{4}\frac{1}{|\det Q|^2}\left(2\operatorname{Re}\left(\overline{\det Q}\ \partial_t(\det Q)\right)\right)\\ &= \frac{\varepsilon}{4}\partial_t\left(\ln|\det Q|^2\right).\end{aligned} \tag{4.11}$$

Integrating Eq. (4.11) from 0 to t leads to Eq. (4.10b). For the real part, we have $\operatorname{Re}\mathcal{B}(C) = \langle\partial_x^2 h\rangle_u - \langle J_A^\top\rangle_u C_\mathrm{R} - C_\mathrm{R}\langle J_A\rangle_u + {C_\mathrm{R}}^2 - {C_\mathrm{I}}^2$ and thus

$$\operatorname{tr}\left(\operatorname{Re}\mathcal{B}(C)C_\mathrm{I}^{-1}\right) = \operatorname{tr}\left(\left(\langle\partial_x^2 h\rangle_u - 2\langle J_A^\top\rangle_u C_\mathrm{R} + ({C_\mathrm{R}}^2 - {C_\mathrm{I}}^2)\right)C_\mathrm{I}^{-1}\right).$$

Combining this with $-\langle h\rangle_u$, we use Lemma A.2 and obtain

$$\begin{aligned}&-\langle h\rangle_u + \frac{\varepsilon}{4}\operatorname{tr}\left(\operatorname{Re}\mathcal{B}(C)C_\mathrm{I}^{-1}\right)\\ &= -\frac{1}{2}\langle(p-A)^2\rangle_u - \langle\phi\rangle_u + \frac{\varepsilon}{4}\operatorname{tr}\left(\langle\partial_x^2 h\rangle_u C_\mathrm{I}^{-1} - 2C_\mathrm{I}\right).\end{aligned}$$

Next, we observe that

$$\begin{aligned}-\frac{1}{2}\langle(p-A)^2\rangle_u + p^\top\langle p-A\rangle_u &= \frac{1}{2}p^\top\langle p-A\rangle_u + \frac{1}{2}\langle A\rangle_u^\top\langle p-A\rangle_u\\ &= \frac{1}{2}v^2 + \langle A\rangle_u^\top v.\end{aligned}$$

Using that $C_\mathrm{I} = (QQ^*)^{-1}$, the real part of the evolution Eq. (4.1c) can thus be written in the claimed form. □

5. Time integration for the equations of motion

In this section we first briefly review the classical Boris algorithm. Afterwards, we present the new Boris-type algorithm and a modification of the classical Runge–Kutta method to solve Eqs. (4.5) and (4.10).

5.1. Boris algorithm for classical equations of motion

The Boris algorithm was originally proposed in [4] for solving the classical equations of motion

$$\dot q = v, \qquad \dot v = v\times B + E, \tag{5.1}$$

for charged particles in an electro-magnetic field. We consider a time-grid t^{nn}, $n \geq 0$, with step size $\tau > 0$. Given approximations $q^n \approx q(t^{nn})$ and $v^{n-\frac12} \approx v(t^{nn-\frac12})$, the algorithm can be written as

$$v^- = v^{n-\frac12} + \frac{\tau}{2}E^n, \qquad E^n = E(t^{nn}, q^n), \tag{5.2a}$$

$$v^+ - v^- = \frac{\tau}{2}\left(v^+ + v^-\right)\times B^n, \qquad B^n = B(t^{nn}, q^n), \tag{5.2b}$$

$$v^{n+\frac12} = v^+ + \frac{\tau}{2}E^n, \tag{5.2c}$$

$$q^{n+1} = q^n + \tau v^{n+\frac12}. \tag{5.2d}$$

Note that the algorithm provides approximations on a staggered grid, where the velocities are only given at half time-steps. Approximations at t^{nn} can be obtained by averaging

$$v^n = \frac{1}{2}\left(v^{n+\frac12} + v^{n-\frac12}\right). \tag{5.2e}$$

Moreover, the scheme is explicit, since one can replace Eq. (5.2b) by

$$v^+ = v^- + \left(v^- + v^-\times\frac{\tau}{2}B^n\right)\times\frac{\tau B^n}{1 + \left|\frac{\tau}{2}B^n\right|^2}, \tag{5.2f}$$

see, e.g., [5]. The Boris algorithm is a second-order method which is not symplectic but conserves the phase-space volume as shown in [11]. A recent analysis was presented in [12].

5.2. Boris-type algorithm

We aim at solving the Euler-Lagrange system Eq. (4.5) together with the two phase Eqs. (4.10a) and (4.10b). The former are closely related to the classical equations of motion of a charged particle Eq. (5.1) except that B is replaced by an averaged field $\langle B\rangle_u$ and that the fields E and SQ do not only depend on q and Q but also in a nontrivial way on v and Υ. While the means $\langle B\rangle_u$ can be approximated by a suitable Gauss-Hermite quadrature formula, evaluating the fields $E = E(t, q, Q, \Upsilon)$ and $S = S(t, q, Q, v, \Upsilon)$ is more involved since they require approximations to v and Υ at time t^{nn}. Unfortunately, these quantities are only defined on the staggered grid $t^{nn\pm\frac{1}{2}}$ and even worse, the update of Υ is coupled to the evaluation of SQ, rendering the scheme implicit.

To be more precise, it is the matrix Υ which is necessary to compute the fields E and S in Lemma 4.1. Averaging Υ as in Eq. (5.2e) would lead to a nonlinear system in $\Upsilon^{n+\frac{1}{2}}$. Therefore, we propose the second-order extrapolation

$$\Upsilon^n = \frac{3}{2}\Upsilon^{n-\frac{1}{2}} - \frac{1}{2}\Upsilon^{n-\frac{3}{2}}, \tag{5.3}$$

and compute also E^n and S^n from it. In our numerical experiments, we saw that using fixed-point iterations to improve the accuracy of Υ^n did not change the errors.

5.3. Discretization of the phase

Motivated by Eq. (4.10b), we define the approximation to $\zeta_{\mathrm{I}}(t^{nn+1})$ as

$$\zeta_{\mathrm{I}}^{n+1} = \zeta_{\mathrm{I}}^{n} + \frac{\epsilon}{2}\Big(\ln\Big|\det Q^{n+1}\Big| - \ln|\det Q^n|\Big). \tag{5.4}$$

This update formula ensures norm preservation of the wave packet.

Lemma 5.1. *Let u^n and u^{n+1} denote two Gaussian wave packets with parameters $(q^n, v^n, Q^n, \Upsilon^n, \zeta^n)$ and $(q^{n+1}, v^{n+1}, Q^{n+1}, \Upsilon^{n+1}, \zeta^{n+1})$, respectively. Then Eq. (5.4) is equivalent to*

$$\|u^n\|_{L^2} = \left\|u^{n+1}\right\|_{L^2}.$$

Proof. Because of

$$\|u^n\|_{L^2}^2 = \exp\big(-\tfrac{2}{\epsilon}\zeta_I^n\big)(\epsilon\pi)^{\frac{d}{2}}|\det Q^n|, \tag{5.5}$$

the norm preservation is equivalent to

$$\exp\big(\tfrac{2}{\epsilon}(\zeta_I^n - \zeta_I^{n+1})\big) = \frac{|\det Q^n|}{\left|\det Q^{n+1}\right|}.$$

This proves the statement. □

Furthermore, for the integration of Eq. (4.10a), we propose to use the midpoint rule with time step size 2τ. This results in a two-step method. Since $v^{n\pm\frac{1}{2}}$ and $\Upsilon^{n\pm\frac{1}{2}}$ are already available, we apply averaging Eq. (5.2e) instead of extrapolation to obtain approximations at t^{nn}. This results in

$$\begin{aligned}\zeta_{\mathrm{R}}^{n+1} = \zeta_{\mathrm{R}}^{n-1} &+ 2\tau\Big(\frac{1}{2}(v^n)^2 + (\langle A\rangle_u^n)^\top v^n - \langle\phi\rangle_u^n\Big)\\ &+ \frac{\epsilon\tau}{2}\operatorname{tr}\big(\langle\partial_x^2 h\rangle_u^n Q^n(Q^n)^* - 2(Q^nQ^{n*})^{-1}\big)\end{aligned} \tag{5.6}$$

5.4. Complete Boris-type algorithm

Overall, combining the time discretization of center, width, and phase of the Gaussian variational wave packet, we get the following algorithm for solving the equations of motion Eqs. (4.5) and (4.10).

Algorithm 1 (One time step with the Boris algorithm). Input: Last steps $(q^n, v^{n-\frac{1}{2}}, Q^n, \Upsilon^{n-\frac{1}{2}}, \zeta^n, \zeta^{n-1})$.

Output: Approximations $(q^{n+1}, v^{n+\frac{1}{2}}, Q^{n+1}, \Upsilon^{n+\frac{1}{2}}, \zeta^{n+1})$.

- compute $q^{n+1}, v^{n+\frac{1}{2}}$ with the Boris algorithm Eq. (5.2) applied to Eq. (4.5a)
- compute $Q^{n+1}, \Upsilon^{n+\frac{1}{2}}$ with the Boris algorithm Eq. (5.2) applied column-wise to Eq. (4.5b),
- compute ζ_{I}^{n+1} and ζ_{R}^{n+1} from Eqs. (5.4) and (5.6), respectively.

In general, one has to apply a Gauss-Hermite quadrature rule to approximate the averages, see [1, Section 8] for details. Note that for strong magnetic fields, filtered variants of the Boris algorithms might be more efficient, cf. [13].

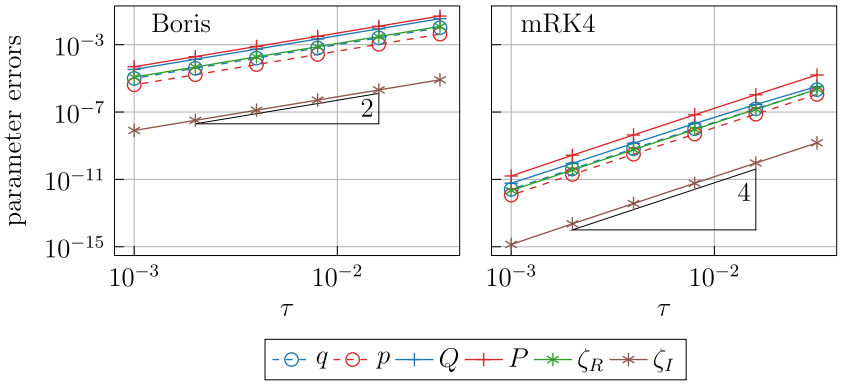

Fig. 2. Simulation of the motion of a particle in a magnetic field in dimension two with potentials Eq. (6.1) and initial values Eq. (6.2). Errors of the numerical solution to Eq. (4.5) approximated by the Boris-type algorithm (left) and the mRK4 method (right) measured in the Frobenius norm scaled with the inverse number of entries. Endtime is chosen as $T = 8$ and $\varepsilon = 10^{-3}$.

5.5. Modified classical Runge–Kutta method

As an alternative to the Boris-type algorithm, we propose a modification of the classical Runge–Kutta method (RK4) of order 4. The modification consists of updating the component ζ_{I} in each intermediate step by using Eq. (5.4) to get the approximations to $\zeta_{\mathrm{I}}(t_{n+1/2})$ and $\zeta_{\mathrm{I}}(t_{n+1})$. All other components are updated by the standard RK4 procedure. In contrast to the original RK4 scheme, the modification automatically conserves the L^2-norm of a Gaussian wave packet.

6. Numerical experiments

In the following section, we present some numerical examples.

6.1. Sublinear magnetic potential in two dimensions

If we consider the potentials

$$A(x,t) = \begin{pmatrix} \sin(x_1 + x_2 + \alpha t) \\ -\sin(x_1 + x_2 + \alpha t) \end{pmatrix}, \qquad \phi(x,t) = \sin(x_1 + x_2) \tag{6.1}$$

with $\alpha \in \{0, 1\}$, we can calculate the occurring averages $\langle A \rangle_u, \langle \phi \rangle_u$ analytically as

$$\begin{aligned} &\int_{\mathbb{R}^d} \sin(x_1 + x_2 + \alpha t)|u(x)|^2 \,\mathrm{d}x \\ &\quad = (\pi\varepsilon)^{d/2} \det(L^{-1}) \exp(-\tfrac{2}{\varepsilon}\zeta_{\mathrm{I}} - \tfrac{\varepsilon}{4}\mathbb{1}^{\top} QQ^{*}\mathbb{1}) \sin(q_1 + q_2 + \alpha t) \end{aligned}$$

where $\mathbb{1} = (1\ 1)^{\top}$ and $(QQ^{*})^{-1} = LL^{\top}$ is the Cholesky decomposition. Since we compare the new time-integrators with the standard RK4 method, which is not norm-conserving, we do not assume normalization of u. We use for the curl of a 2d vector potential A the convention $\nabla \times A = \partial_1 A_2 - \partial_2 A_1$. Initial values are chosen as

$$q^0 = \begin{pmatrix} 0 \\ 0 \end{pmatrix}, \quad p^0 = \begin{pmatrix} 1 \\ 0 \end{pmatrix}, \quad Q^0 = \begin{pmatrix} 1 & 0 \\ 0 & 1 \end{pmatrix}, \quad P^0 = \begin{pmatrix} \mathrm{i} & 0 \\ 0 & \mathrm{i} \end{pmatrix}, \quad \zeta_{\mathrm{R}}^0 = 0. \tag{6.2}$$

The imaginary part of the phase ζ_{I}^0 is chosen such that the corresponding initial Gaussian wave packet u^0 is normalized. Note that the normalization is ε dependent and thus the initial value ζ_{I}^0 changes for different values of ε.

In Fig. 2 we depict the maximal component errors over all time steps of a Gaussian wave packet where we solve Eq. (4.5) with the Boris-type Algorithm 1 (left) and the modified fourth order Runge–Kutta (mRK4) method (right). As end time we choose $T = 8$ and set $\alpha = 1, \varepsilon = 10^{-3}$. We compare the numerical solution to a reference solution calculated by the standard RK4 method applied to Eqs. (4.1) and (4.2) with time step-size $\tau = 10^{-4}$. As we see, the error decreases by order two for the Boris-type method and by order four for the mRK4 method with decreasing time step-size.

In Fig. 3 we illustrate the maximal L^2-error over all time steps of a Gaussian wave packet with parameters calculated by the Boris-type method (left) and a Gaussian wave packet with parameters calculated by the mRK4 method (right). Again we compute the error against a reference solution calculated with the standard RK4 method applied to Eqs. (4.1) and (4.2) with time stepsize $\tau = 10^{-4}$. The L^2-norm between the two Gaussian wave packets is computed with a Gauss–Hermite quadrature rule. We see a reduction of order two for the Boris-type method and of order four for the mRK4 method in the L^2-norm. Moreover, we see that the error constant scales as ε^{-1} in both cases, which is supported by the theoretical result [1, Thm. 7.7]. Further note that the L^2-error between two

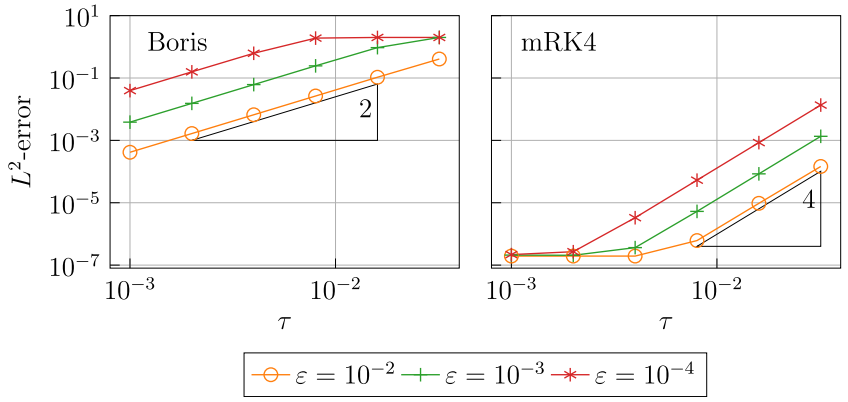

Fig. 3. L^2-error of a Gaussian wave packet approximated by the Boris-type method Eq. (1) (left) and the mRK4 method (right) against a reference Gaussian wave packet with coefficients approximated by the classical RK4 method with time stepsize $\tau = 10^{-4}$. The potentials are given by Eq. (6.1) and the initial values by Eq. (6.2). Different values for ε are considered. Endtime is chosen as $T = 8$.

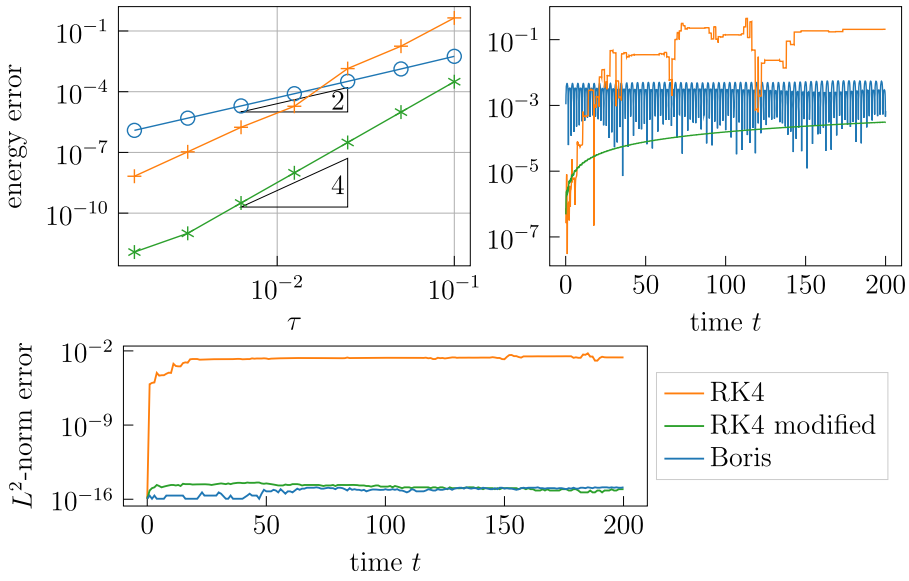

Fig. 4. Energy error against the initial energy (top) and L^2-norm error (bottom) using the potentials and initial values in Section 6.1. The endtime is chosen as $T = 200$ and $\varepsilon = 10^{-3}$. On the left, the maximal energy error is illustrated over all time stamps for different time stepsizes τ. On the right, the energy error over the time interval $[0, 200]$ is plotted for a fixed time stepsize $\tau = 10^{-1}$.

normed Gaussian wave packets is bounded by 2, which explains the upper plateau in the left plot. The lower plateau in the right plot corresponds to the numerical computation of the underlying integral at almost machine precision.

In Fig. 4 we compare the error between the energy Eq. (A.1) and the initial energy (top) of a Gaussian wave packet between the three methods, Boris-type, mRK4, and standard RK4. We have fixed $\alpha = 0$ in Eq. (6.1) such that we have time-independent potentials and therefore theoretical energy conservation. As end time we chose $T = 200$ and $\varepsilon = 10^{-3}$. On the left, we plot the maximal energy error at each time stamp to the initial energy for different time step-sizes τ. We see a reduction of order two of the error for the Boris-type method and of order four for the mRK4 and standard RK4 methods. Note, however, that the error of the standard RK4 method is several powers of ten worse than that of the mRK4 method. In comparison to the Boris-type method, the error of the RK4 method is much larger for larger values of τ but due to the higher order of error reduction of the RK4 method the lines intersect at some point. Therefore, for larger values of τ the Boris-type method outperforms the RK4 method. In the right plot, we plot the energy error against the initial error at each time stamp for a fixed time step-size $\tau = 10^{-1}$. As we see, the error of the Boris-type method oscillates at the same level, while we see for the standard RK4 and mRK4 methods a drift. Note, however, that the drift of the mRK4 method is way smaller than that of the standard RK4 method. Moreover, at the bottom of Fig. 4 we illustrate the error of the L^2 norm of a Gaussian wave packet to norm conservation using time step-size $\tau = 10^{-1}$. The error for the Boris-type method and the mRK4 method is close to the machine precision and hence shows conservation of the L^2-norm, whereby using the standard RK4 method results in a deviation. The L^2-norm of a Gaussian wave packet given its parameters can be calculated analytically by Eq. (5.5).

Table 2
L^2-norm error and error with respect to the L^2-norm between the exact solution using the potentials Eq. (2.1) with data given in Table 1 and initial values Eq. (6.3) and the numerical solution u^n by the mRK4 method measured at endtime $T = 2\pi$.

step-size τ	$2.5 \cdot 10^{-5}$	10^{-5}	$5.0 \cdot 10^{-6}$
$\left\lvert \lVert u^n \rVert_{L^2} - \lVert \psi(t^n) \rVert_{L^2} \right\rvert$	$1.6 \cdot 10^{-10}$	$2.6 \cdot 10^{-10}$	$3.4 \cdot 10^{-10}$
$\lVert u^n - \psi(t^n) \rVert_{L^2}$	$8.0 \cdot 10^{-3}$	$1.9 \cdot 10^{-4}$	$5.6 \cdot 10^{-6}$

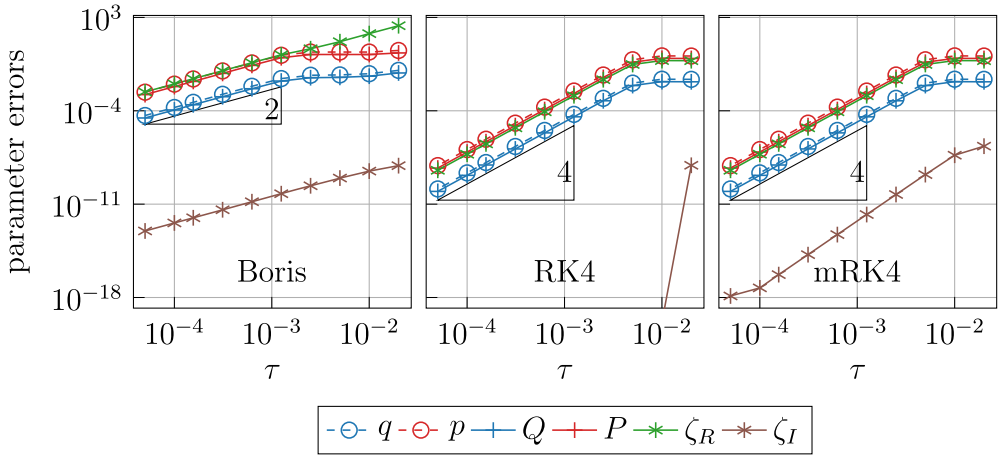

Fig. 5. Maximum errors of the parameters approximated by the Boris-type method Eq. (1) (left), the RK4 method (middle) and the mRK4 method (right) against the exact solution using the potentials Eq. (2.1) with data given in Table 1 and initial values Eq. (6.3). Measured in the Frobenius norm scaled with the inverse number of components. Endtime is chosen as $T = 2\pi$.

6.2. Penning trap

As a second example, we apply the time-integrators to the three–dimensional quantum dynamics of a proton in a hyperbolic Penning trap, see Section 2. We consider the Schrödinger Eq. (2.3) with the trap parameters of Table 1 and an initial Gaussian wave packet with parameters (in dimensionless units)

$$\begin{aligned} q^0 &= \begin{pmatrix} 0.133 & 0.133 & 0.258 \end{pmatrix}^\top, \quad Q^0 = \operatorname{diag}(q^0), \\ p^0 &= \begin{pmatrix} 0.133 & 7.492 & 3.879 \end{pmatrix}^\top, \quad P^0 = \mathrm{i} \cdot (Q^0)^{-1}, \\ \zeta^0 &= 1.009 - 1.84 \cdot 10^{-7}\mathrm{i}. \end{aligned} \tag{6.3}$$

The initial condition is chosen such that the dynamics are coherent in the sense, that the width of the packet does not change over time. The phase parameter has a non-vanishing real part to be aligned with the analytic expressions for the center motion that were recently given in [14, eqs. (12) and (17)] (with $\omega_\perp = \Omega/2$). As previously mentioned, see for example Section 3.2, the variational approximation is exact in this case, such that the observed numerical error is only due to the time integrator. In Table 2, we list both the L^2-norm error $\left\lvert \lVert u^n \rVert_{L^2} - \lVert \psi(t^n) \rVert_{L^2} \right\rvert$ and the error with respect to the L^2-norm $\lVert u^n - \psi(t^n) \rVert_{L^2}$ between our numerical solution and the exact analytical solution by the mRK4 method measured at the end time $T = 2\pi$ for some time step-sizes τ. The proof of [1, Theorem 7.7] literally also applies here and implies that the error in the L^2-norm scales with $\varepsilon^{-1} \approx 10^8$. Hence, even if we choose the time step-size small enough to reach machine precision for the parameters of the Gaussian wave packet, there is an accuracy bound for this error measure. Moreover, due to the square-root in the calculation of the L^2-norm, we also cannot meet machine precision in this respect as was already mentioned in Section 6.1. The numerical time evolution does not require averages but only point evaluations, see Remark 1. In this set-up, we see the exact errors of our numerical schemes to integrate the equations of motion Eqs. (4.5) and (4.10).

In Fig. 1, we showed the exact trajectory of the position center. Virtually the same trajectory is obtained by our numerical simulations for $\tau \lesssim 10^{-3}$, as confirmed by the small errors illustrated in Fig. 5.

There, we present the maximal error over all time steps of the parameters against the exact solution for different step-sizes τ in the Frobenius norm scaled by the inverse number of the components. As expected, the Boris-type method converges with order two while the RK4 and mRK4 methods converge with order four. We are convinced that the plateau at larger time step-sizes occurs since the parameter evolution is mildly oscillatory because the quotients $\omega_+/\omega_- \approx 113.25$ and $B/B_m \approx 114.25$ of the potentials in Eq. (2.3) are not small, and since we did not observe such plateaus when setting these quotients close to one. Moreover, the error for the

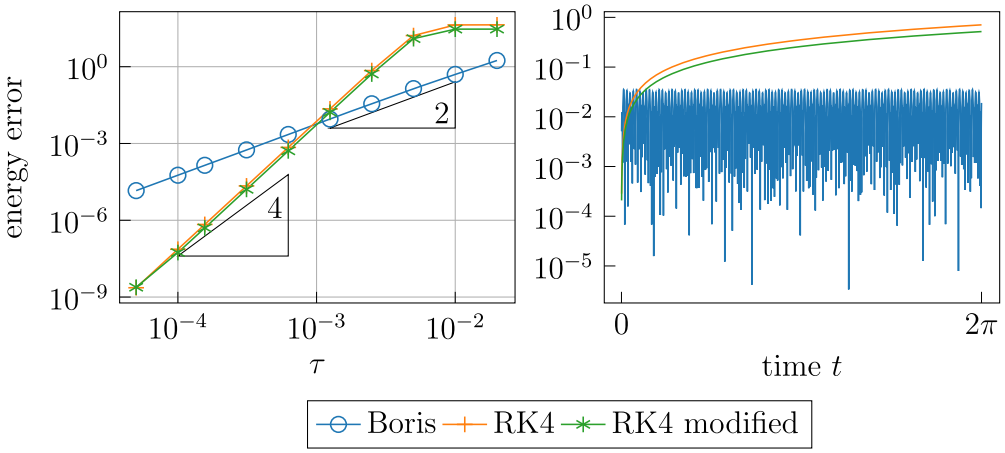

Fig. 6. Energy error using the potentials Eq. (2.1) and initial values Eq. (6.3). The endtime is chosen as $T = 2\pi$. On the left, the maximal energy error is plotted for different time step-sizes τ. On the right, we plotted the energy error over time for $\tau = 2.5 \cdot 10^{-3}$.

imaginary phase ζ_I using the RK4 method applied to Eq. (4.1) is close to the machine precision since the exact solution is constant. In contrast, in the mRK4 method, the error of ζ_I directly relates to the error of Q by Eq. (5.4) and thus shows order four. Finally, in Fig. 6 we compare the maximal energy error over all time steps of the three methods, which shows a drift for the RK4 methods but not for the Boris-type algorithm.

CRediT authorship contribution statement

Malik Scheifinger: Writing – review & editing, Writing – original draft, Visualization, Validation, Software, Project administration, Methodology, Investigation, Formal analysis, Data curation, Conceptualization; **Kurt Busch:** Writing – review & editing, Writing – original draft, Visualization, Validation, Supervision, Project administration, Methodology, Investigation, Formal analysis, Conceptualization; **Marlis Hochbruck:** Writing – review & editing, Writing – original draft, Visualization, Validation, Supervision, Project administration, Methodology, Investigation, Funding acquisition, Formal analysis, Conceptualization; **Caroline Lasser:** Writing – review & editing, Writing – original draft, Visualization, Validation, Supervision, Project administration, Methodology, Investigation, Funding acquisition, Formal analysis, Conceptualization.

Data availability

The link to all codes is given in the manuscript.

Declaration of competing interest

The authors declare that they have no known competing financial interests or personal relationships that could have appeared to influence the work reported in this paper.

Acknowledgments

The collaboration among the authors was inspired by discussions during the Workshop “Nonlinear Optics: Physics, Analysis, and Numerics” at Mathematisches Forschungsinstitut Oberwolfach. We are thankful to the institute for creating such a pleasant and stimulating atmosphere. We thank Selina Burkhard for co-supervising the Master thesis of Malik Scheifinger, which was the origin of this project. Funded by the Deutsche Forschungsgemeinschaft (DFG, German Research Foundation) – Project-ID 258734477 – SFB 1173 and – Project-ID 470903074 – TRR 352.

Appendix A. Appendix: Gaussian calculus and energy formula

Lemma A.1. *Consider smooth functions $W : \mathbb{R}^d \to \mathbb{C}^{d\times d}$ and $w : \mathbb{R}^d \to \mathbb{C}$, and an arbitrary matrix $M \in \mathbb{C}^{d\times d}$. Let $u \in L^2(\mathbb{R}^d)$ be a Gaussian wave packet with position q and width $C = C_R + iC_I$. Then,*

$$\langle W(x-q)\rangle_u = \frac{\varepsilon}{2}\sum_{\ell=1}^{d}\left(\left(\langle \partial_\ell W\rangle_u C_I^{-1}\right)_{k\ell}\right)_{k=1}^{d},$$

$$\langle (x-q)^\top w M (x-q)\rangle_u = \frac{\varepsilon}{2}\langle w\rangle_u \operatorname{tr}\left(MC_I^{-1}\right) + \frac{\varepsilon^2}{4}\operatorname{tr}\left(\langle \nabla^2 w\rangle_u C_I^{-1} M C_I^{-1}\right).$$

In particular, $\langle w(x-q)\rangle_u = \frac{\varepsilon}{2} C_{\mathrm{I}}^{-1} \langle \nabla w \rangle_u$.

Proof. The position density

$$|u(t,x)|^2 = \exp\Big(-\frac{1}{\varepsilon}(x-q)^\top C_{\mathrm{I}}(x-q) - \frac{2}{\varepsilon}\zeta_{\mathrm{I}}\Big)$$

satisfies $\nabla |u(t,x)|^2 = -\frac{2}{\varepsilon} C_{\mathrm{I}}(x-q)|u(t,x)|^2$. Therefore, partial integration yields that

$$\begin{aligned}\langle W(x-q)\rangle_u &= -\frac{\varepsilon}{2}\int_{\mathbb{R}^d} W(x)\, C_{\mathrm{I}}^{-1}\nabla |u(t,x)|^2 \,\mathrm{d}x \\ &= \frac{\varepsilon}{2}\sum_{\ell=1}^{d} \big(\langle \partial_\ell (W C_{\mathrm{I}}^{-1})_{k,\ell}\rangle_u\big)_{k=1}^{d}.\end{aligned}$$

Similarly, two partial integrations imply that

$$\begin{aligned}\langle w(x-q)^\top M(x-q)\rangle_u &= \sum_{k,\ell=1}^{d} \Big\langle w(C_{\mathrm{I}}(x-q))_k (C_{\mathrm{I}}^{-1} M C_{\mathrm{I}}^{-1})_{k\ell} (C_{\mathrm{I}}(x-q))_\ell \Big\rangle_u \\ &= \frac{\varepsilon}{2}\sum_{k,\ell=1}^{d} \big(\langle w\rangle_u (C_{\mathrm{I}})_{k\ell} + \big\langle \partial_\ell w (C_{\mathrm{I}}(x-q))_k \big\rangle_u\big)(C_{\mathrm{I}}^{-1} M C_{\mathrm{I}}^{-1})_{k\ell} \\ &= \sum_{k,\ell=1}^{d} \Big(\frac{\varepsilon}{2}\langle w\rangle_u (C_{\mathrm{I}})_{k\ell} + \frac{\varepsilon^2}{4}\big\langle \partial_k \partial_\ell w\big\rangle_u\Big)(C_{\mathrm{I}}^{-1} M C_{\mathrm{I}}^{-1})_{k\ell} \\ &= \frac{\varepsilon}{2}\langle w\rangle_u \operatorname{tr}(M C_{\mathrm{I}}^{-1}) + \frac{\varepsilon^2}{4}\operatorname{tr}(\langle \nabla^2 w\rangle_u C_{\mathrm{I}}^{-1} M C_{\mathrm{I}}^{-1}).\end{aligned}$$

□

Lemma A.2. *Let u be a normalized Gaussian wave packet with center (q,p) and width $C = C_{\mathrm{R}} + \mathrm{i}C_{\mathrm{I}}$. Then it holds for the energy*

$$\langle H\rangle_u = \frac{1}{2}p^2 - p^\top \langle A\rangle_u + \frac{1}{2}\langle A^2\rangle_u + \langle \phi\rangle_u + \frac{\varepsilon}{4} R_H \tag{A.1}$$

with remainder

$$R_H = \operatorname{tr}\big(\big({C_{\mathrm{R}}}^2 + {C_{\mathrm{I}}}^2 - 2\langle J_A^\top\rangle_u C_{\mathrm{R}}\big) C_{\mathrm{I}}^{-1}\big).$$

If the magnetic potential A is linear in x, then $\langle A\rangle_u = A(q)$ and

$$\langle A^2\rangle_u = A(q)^2 + \frac{\varepsilon}{2}\operatorname{tr}\big(J_A(q)^\top J_A(q) C_{\mathrm{I}}^{-1}\big) \tag{A.2}$$

Proof. In the following, we ignore the dependence on t to simplify the notation. Since $\langle H\rangle_u = \langle h\rangle_u = \frac{1}{2}\langle(\xi - A)^2\rangle_u + \langle\phi\rangle_u$, we only need to work on the mean of $\mathrm{op}_{\mathrm{Weyl}}((\xi - A)^2) = (\mathrm{op}_{\mathrm{Weyl}}(\xi - A))^2$. We have

$$\begin{aligned}&\langle(\xi - A)^2\rangle_u = \langle(\xi - A)u, (\xi - A)u\rangle \\ &= \langle(C(x-q) + (p - A))u, (C(x-q) + (p-A))u\rangle \\ &= \langle (x-q)^\top C^* C (x-q)\rangle_u + \langle (p-A)^\top (C + C^*)(x-q)\rangle_u + \langle (p-A)^2\rangle_u \\ &= \frac{\varepsilon}{2}\operatorname{tr}(C^* C C_{\mathrm{I}}^{-1}) - \frac{\varepsilon}{2}\operatorname{tr}(\langle J_A^\top\rangle_u (C + C^*) C_{\mathrm{I}}^{-1}) + \langle (p-A)^2\rangle_u\end{aligned}$$

due to Lemma A.1. For the traces, we have

$$\begin{aligned}&\operatorname{tr}(C^* C C_{\mathrm{I}}^{-1}) = \operatorname{tr}((C_{\mathrm{R}} - \mathrm{i}C_{\mathrm{I}})(C_{\mathrm{R}} + \mathrm{i}C_{\mathrm{I}}) C_{\mathrm{I}}^{-1}) = \operatorname{tr}(({C_{\mathrm{R}}}^2 + {C_{\mathrm{I}}}^2) C_{\mathrm{I}}^{-1}) \\ &\operatorname{tr}(\langle J_A^\top\rangle_u (C + C^*) C_{\mathrm{I}}^{-1}) = 2\operatorname{tr}(\langle J_A^\top\rangle_u C_{\mathrm{R}} C_{\mathrm{I}}^{-1}).\end{aligned}$$

Combining the terms, we obtain Eq. (A.1). In the linear case, we expand $A(x) = A(q) + J_A(q)^\top (x-q)$ and use Lemma A.1 to prove Eq. (A.2). □

References

[1] C. Lasser, C. Lubich, Computing quantum dynamics in the semiclassical regime, Acta Numer. 29 (2020) 229–401. https://doi.org/10.1017/s0962492920000033

[2] J. Vanicek, Family of Gaussian wavepacket dynamics methods from the perspective of a nonlinear Schrödinger equation, J. Chem. Phys. 159 (1) (2023) 014114. https://doi.org/10.1063/5.0146680

[3] S. Burkhard, B. Dörich, M. Hochbruck, C. Lasser, Variational Gaussian approximation for the magnetic Schrödinger equation, J. Phys. A Math. Theor. 57 (29) (2024) 295202. https://doi.org/10.1088/1751-8121/ad591e

[4] J.P. Boris, Relativistic plasma simulation-optimization of a hybrid code, in Proceeding of Fourth Conference on Numerical Simulations of Plasmas (1970) 3–67. https://apps.dtic.mil/sti/citations/ADA023511.

[5] C.K. Birdsall, A.B. Langdon, Plasma Physics via Computer Simulation, CRC Press, 2018. https://doi.org/10.1201/9781315275048.

[6] L.S. Brown, G. Gabrielse, Geonium theory: physics of a single electron or ion in a penning trap, Rev. Mod. Phys. 58 (1) (1984) 233–311. https://doi.org/10.1103/RevModPhys.58.233

[7] M. Vogel, Particle Confinement in Penning Traps, 126 of *Sringer Series on Atomic, Optical, and Plasma Physics*, Springer, Cham, 2024. An Introduction. https://doi.org/10.1007/978-3-031-55420-9
[8] M. Kretzschmar, Octupolar excitation of ion motion in a penning trap: a theoretical study, Int. J. Mass Spectrom., 357 (2014) 1–21. https://doi.org/10.1016/j.ijms.2013.09.007
[9] C. Lubich, From quantum to classical molecular dynamics: reduced models and numerical analysis, Zurich Lectures in Advanced Mathematics, European Mathematical Society (EMS), Zürich, 2008. https://doi.org/10.4171/067
[10] D. Robert, M. Combescure, Coherent states and applications in mathematical physics, Theoretical and Mathematical Physics, Springer, Cham, 2021. Second edition [of 2952171]. https://doi.org/10.1007/978-3-030-70845-0
[11] H. Qin, S. Zhang, J. Xiao, J. Liu, Y. Sun, W.M. Tang, Why is Boris algorithm so good?, Phys. Plasmas 20 (8) (2013). https://doi.org/10.1063/1.4818428
[12] E. Hairer, C. Lubich, Long-term analysis of a variational integrator for charged-particle dynamics in a strong magnetic field, Numer. Math. 144 (3) (2020) 699–728. https://doi.org/10.1007/s00211-019-01093-z
[13] E. Hairer, C. Lubich, B. Wang, A filtered Boris algorithm for charged-particle dynamics in a strong magnetic field, Numer. Math. 144 (4) (2020) 787–809. https://doi.org/10.1007/s00211-020-01105-3
[14] I. Bialynicki-Birula, Z. Bialynicka-Birula, Classical-quantum correspondence for particles in the penning trap, Phys. Scr. 99 (4) (2024) 045103. https://doi.org/10.1088/1402-4896/ad2c43